SSRG International Journal of Civil Engineering
ISSN: 2348-8352/ https://doi.org/10.14445/23488352/IJCE-V13I2P108

Volume 13 Issue 2, 101-116, February 2026

Original Article

Analysis of the Influence of Sky View Factor on the Thermal Environment of Coastal Settlements in Gorontalo City based on IoT Measurements

Amru Siola[1], Baharuddin Hamzah[2], Rosady Mulyadi[3], Nurul Jamala[4]

[1,2,3,4]*Department of Architecture, Faculty of Engineering, Hasanuddin University, Gowa 92171, Indonesia.*

[2]*Corresponding Author : baharsyah@unhas.ac.id*

Received: 18 November 2025 Revised: 19 December 2025 Accepted: 20 January 2026 Published: 11 February 2026

Abstract *- Tropical coastal urban areas are highly vulnerable to climate-induced stress, and thus, a process-based understanding of how the urban morphology regulates microclimate and thermal comfort is required. This paper assesses the impact of SVF on the thermal environment at a coastal settlement in Gorontalo City, Indonesia, by using IoT-integrated measurements and residents' thermal perception data. Measurements were made at six paired field sites along a Coastal Foothill Transect (T0-T5), using IoT-based monitoring of temperature, humidity, and wind speed, combined with hemispherical photography and savannah view factor estimation from Google Street View. Statistical methods such as ANOVA, multivariate regression, and robust regression were used to correlate objective thermal indices (Ta, PMV, PET) with subjective responses (TSV, Acceptability). The results indicate that low SVF is associated with higher temperature (+2-6 °C), elevated heat perception (TSV +1,7-2,1), and reduced acceptability (≥ 0.76). The mulivariate model (R2adj = 0.84) confirms that SVF primarily influences thermal comfort through airflow regulation rather than direct temperature control. These findings provide rare field-based evidence from a humid tropical coastal control context and highlight SVF as a critical morphological parameter for climate-responsive urban design.*

Keywords *- Sky View Factor, Thermal Comfort, Coastal Settlements, Internet of Things, Climate Adaptive, Gorontalo City.*

1. Introduction

The effects of rising global temperatures and the increase in UHI was of special before their time" (to quote The Beatles) due to the influence of urban development that focus on thermal conditions, both internationally and locally [1, 2] This sensitivity must be further studied with exceptionalta importance for studies environmental predictions The problem affects the standard of living for inhabitants but also public health, energy conservation and urban regulation. In tropical atmospheres, the need for solar radiation is very high throughout the year. High air humidity also presents obstacles to achieving outdoor thermal comfort. There are relatively few studies on the influence of these climatic factors on outdoor thermal conditions and possible improvement measures [6, 7].

'Outdoor Thermal Comfort' is primarily described as facility-related to the UHI phenomenon [8]. It was defined on the human satisfaction with the joint operation of physical and climate factors [9] as thermal comfort. Human feeling of thermal comfort is affected by four factors: air temperature, radiation temperature, humidity, and wind speed [10], and also individual factors such as clothing and activity level [11]. In tropical environments, people prefer to seek out areas with lower temperatures [12]. Buildings in densely built-up tropical coastal residential areas that extend across land are believed to block narrow road corridors and impede plantation, thereby obstructing air flow. These conditions can also result in increased surface heating.

This study aims to investigate how these spatial forms specifically impact urban microclimates in tropical coastal settings [13, 14]. These factors directly impact the thermal environment by affecting air temperature, relative humidity, and wind speed, which collectively influence the overall thermal environment. The main research question is how these factors exert their influence. One indicator of the influence of spatial geometry on thermal conditions is the Sky View Factor (SVF), which is the proportion of the sky visible from a given observation point. A higher SVF generally allows for increased heat loss and solar gain, directly impacting local thermal conditions [15-18]. Although SVF has been extensively studied in urban contexts, quantitative studies on its impact on thermal parameters in tropical coastal settlements, particularly those incorporating real-time technology-based measurements, remain limited [19, 20].

Several approaches can be used to measure SVF, which influences variables such as thermal comfort and radiation exposure, including geometric calculation methods, satellite image analysis, and fisheye photography (also known as hemispheric photography) [21, 22].

Fisheye photography provides accurate visual data. Segmentation algorithms clearly separate sky and non-sky areas, yielding precise SVF values. Combined with IoT-based microclimate monitoring, this method yields detailed spatial-temporal data that clarifies the specific impact of Sky View Factor (SVF) on the link between spatial morphology and thermal conditions [23, 24].

Previous research has shown that SVF values significantly impact air temperature, humidity, and overall comfort levels. [15, 25]. Indeed, the majority of existing studies have been based in temperate regions or non-coastal, dense urban areas; a study that integrates fisheye photography-based SVF analysis and IoT monitoring in a tropical coastal context, especially from the Indonesia side, is uncommon. Hence, this work has two primary roles: (1) to study the effect of SVF on thermal conditions in coastal communities by integrating fisheye derived SVF and real-time monitoring of temperature in Gorontalo City; and (2) to investigate how urban microclimate changes with seasons using the Envi-met model [26] during an academic semester based on a university's campus situated in humid subtropical zones.

There are several studies that have focused on the correlation between Sky View Factor (SVF) and thermal comfort; however, not many of them involve the use of fisheye photography and IoT-based monitoring at tropical coastal areas. To fill this research gap, the current study investigates the impact of SVF on the coastal thermal environment in Gorontalo City based on calibrated fisheye satellite-based SVF measurements and real-time data IoT monitoring.

There is now an urgent need for this research as its outcomes may inform the development of a real-time adaptive spatial planning model wherein sky openness could be considered as a key variable for mitigating urban heat. The results of the study are expected to aid in evidence-based urban design policies that enhance thermal comfort in tropical coastal areas that experience local and global climate pressures.

The novelty of this study lies in the following aspects:

- The integration of Sky View Factor (SVF) with airflow mechanisms is a primary regulator of thermal comfort.
- The combination of multi-source, field-based SVF measurements;
- The application of real-time IoT monitoring in tropical coastal settlements, and
- The development of a spatially adaptive model to support planning in tropical coastal areas.

2. Literature Review

2.1. Concept and Measurement of Sky View Factor

The Sky View Factor (SVF) is the ratio of the sky patch area visible from a point on the surface to the whole hemisphere of unobstructed visible sky [27]. SVF is commonly used to describe the angular openness of an outdoor space to solar radiation heat loss and air flow [28]. Measurement techniques included the type of Nikon camera used (DS1X-HR), urban climate modeling RX-AX 53 between un-shadowed areas, and the site shadow ratio [29] introduced the concept of a footprint for SVF that combines hemispheric image analysis with Urban Climate Modeling to arrive at a spatially distributed representative value for SVF based on mathematical representation of hue, or fisheye photography techniques.

2.2. The Relationship of SVF to Thermal Conditions in Tropical Climates

Physiologically relevant in the tropics, SVF serve double duty: high values increase daytime heat load by admitting more solar radiation , whereas low values impede ventilation and retard nocturnal cooling [30]. Improving sky openness in street layouts and even open spaces, such as with the creation of shade-inducing trees in tropical cities [31].

2.3. Calculation SVF

Modified Steyn's method used for SVF computation [32]. In a photograph taken with the convex fisheye lens, only 36 separate ring-shaped circles. The contributions of each ring are summed to obtain the SVF. A detailed yet straightforward approach in terms of the contribution of each ring to the overall SVF calculation.

$$SFV = \frac{\pi}{2n} \sum_{i=1}^{n} sin\left(\frac{\pi\,(2i-1)}{2n}\right)\left(\frac{p_i}{t_i}\right) \quad (1)$$

Output:

- n = area of the ring circle fisheye photo
- p_i/t_i = the ratio between the total number in the ring

SVF categories are defined in three levels:

a. High SVF: open area with minimal obstructions (example T0)
b. Low SVF: narrow urban canyon with major obstacles (example T3)
c. Medium Low SVF: narrow roads with varying openness (example T1, T2, T4, T5)

2.4. The Role of IoT in Microclimate Monitoring

Recently, the affordable, real-time monitoring of microclimate parameters over large scales and wide time spans has become possible due to (IoT/IoE), advancing our capability in investigating and controlling local environmental conditions [33]. IoT devices are able to measure air temperature, relative humidity, and wind speed in high levels of detail. This enables straightforward comparison of thermal conditions and morphological parameters such as SVF.

Applying IoT in combination with the image-based SVF measurement technique facilitates more accurate and evidence-based research.

2.5. Research Gap and Position of this Study

While there are a number of studies that have examined SVF and thermal comfort, few use fisheye photography combined with IoT measurements in tropical coastal locations. These data are collected by means of calibrated fisheye SVF measurement and real-time IoTey, the influence of SVF in Gorontalo City on coastal thermal environmental monitoring. Many studies have researched thermal environments. Nevertheless, to facilitate the discussion and minimize overtly redundant interpretations, in this study, we do so by distinguishing ourselves from previous studies on several fronts (see below):

Thermal Comfort Models Mainstream models of the world, PMV (Fanger), Adaptive ASHRAE, and PET/UTCI, etc., are predominantly from subtropical climates and indoor conditions; hence, less appropriate for us in humid tropics, especially on the coast (de Dear et al., 2020; Yang et al., 2021). Research novelty The added value of this research is to develop the Coastal Thermal Comfort Model with local reference to a humid tropical climate and the Indonesian coastal metro district (locally Gorontalo). Environmental and Morphology Factors: Most previous studies only concerned land use change (such as a decrease of green open space, loss of water infiltration areas) at the urban scale. Often, it is not described how the measurements were taken. They also commonly tend to establish a connection between the decreasing standards of living conditions and the transformation of green areas into new settlements (Anriani, 2024). Research status: This work incorporates microclimatic

Measurement Methodology: The majority of previous studies still rely on manual (snapshot-based) measurements with data limited to specific time periods. Real-time spatial–temporal monitoring remains rarely applied in humid tropical coastal settlements (Gupta et al., 2022; Rahman et al., 2023). Research distinction: This study applies IoT-based sensors with real-time monitoring to obtain continuous spatial–temporal thermal data at six measurement points within the coastal settlements of Gorontalo City.

3. Materials and Methods

3.1. Study Area

Thermal Comfort Models: Current global models, such as PMV (Fanger), Adaptive ASHRAE, and PET/UTCI, still have a subtropical or cold indoor condition bias and are not suitable for humid conditions. This research was carried out in Pohe Village, Gorontalo City, located on the coast of Gorontalo Bay with a tropical climate. The area presents a standard coastal settlement: medium to high building density, narrow alleys, and an H/W ratio bigger than in some parts, with an uneven distribution of vegetation. At some point, the vegetation exists (e.g., beach trees in T0 and mango trees in T3), whereas at others the location is more open, without shading. Climatologically, the region has an average annual temperature between 28 and 32 °C and relative humidity between 70 and 80 %. Given these spatial constraints and the ambient conditions, this is a suitable context to model thermal comfort that combines morphology and microclimate input parameters. Furthermore, the SVF is highly variable across the observed points, which is related to microclimate differences.

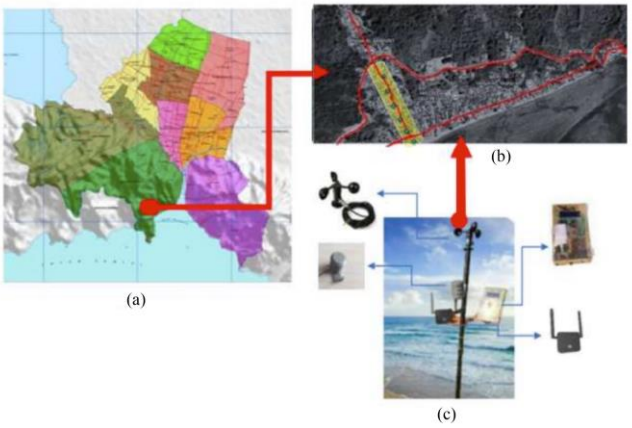

Fig. 1 (a) Gorontalo City Map, (b) Pohe's Research Location, Hulonthalangi District, and (c) IoT-based Sensor (temperature, humidity, and wind speed)

3.2. Determination of Measurement Points and Research Period

Six Observation Levels (T0-T5) were established along a line connecting the lakeshore to foothillet, spaced approximately 50 m apart from each other, for evaluation of microclimate. The random point distribution is meant to reflect the diversity of morphological and environmental conditions in Pohe Suddistrict. The plan is structured in three characteristic areas: an open beach area influenced by sea breezes; a closely built center with partial greenery, but limited sky-visibility, and a friction area next to the hill that is partially shaded.

Even though just a few sites were recorded, this system is helpful to show how the microclimatic characteristics of tropical coastal settlements change gradually through space. The selection of sites along this coast-hill transect allows clear conclusions regarding the influence of morphological diversity on microclimate over minor spatial gradients.

The data gathered for air temperature, relative humidity, and wind speed were collected in June–July 2025, coinciding with the seasonal shift from the rainy to dry period in Gorontalo. This date range was selected to include typical temperature conditions during peak solar radiation, minimal rainfall, and increased outdoor human activity. Despite the single season of observation, this dataset offers a valid and contextually relevant insight into how thermal comfort is

dynamically experienced by residents in the Pohe coastal environment.

3.3. SVF Mesurement

The Sky View Factor (SVF) is the proportion between visible sky area from a surface point and the whole half-sphere unobstructed visible [27]. SVF has been widely accepted as an indicator of the degree to which outdoor spaces are open (i.e., exposed to solar heat gain and loss as well as air movement) [35]. In connection with these, there are measurement methods based on geometry and analytical methods, as well as using photographic images taken with the use of fisheye photography. Also presented the SVF footprint: a framework to integrate hemispheric image analysis and urban climate modeling for a citywide representative SVF value. SVF was monitored at six observation stages (T0–T5) located 50 m apart from the shoreline to the land area in this study. Hemispherical photographs were acquired at each site with a digital camera mounted on a vertical 1.5 m tall tripod equipped with a 180° fisheye lens.

SVF analysis uses two approaches. The evaluations from field observations are derived from the openness of the sky, which is evaluated according to building density, vegetation, and orientation of roads. The second stage processes the GSV images with a Conversion Neural Network (CNN)-based model to separate sky building [36, 37]. Finally, the predictions from the two methods are validated at sampled points against hemispherical fisheye photos.

3.4. IoT Monitoring

The microclimate parameters were recorded by an IoT (Internet of Things)-based sensor system positioned at each point: T0—T5. The sensor records three main variables:

- Air temperature (Ta): uses a thermistor sensor with an accuracy of ±0,3 equipped with an aspirated radiation shield.
- Relative humidity (RH): measured by a capacitance sensor with an accuracy of ±2%.
- Wind speed (v): measured with an ultrasonic anemometer (accuracy ±0,1 m/s) installed at a height of 1,5-2 m.

All sensors are interoperated using Hypertext Transfer Protocol Secure (HTTPS), allowing real-time data transfer to the server. The method of down's co-location is used to check the consistency among sensors. 24 hours in this mode for 24 hrs before it was installed at the measurement point. The data is acquired in increments of one minute with a 10-minute running average to minimize noise.

3.5. Thermal Comfort Analysis

Thermal sensation was determined in accordance with the PMV index, which was initially developed by Fanger and standardized in ASHRAE 55 [38] and ISO 7730. The PMV model uses several input parameters: the air Temperatures (Ta), Mean Radiant Temperature (Tg) or Black Globe Tempera- Ture, Relative Humidity (RH) and Air Velocity v. Standard Metabolic Rate (Metabolic rate known as M; 24 W/m is the standard resting metabolic rate), Clothing Insulation Values (cloths) were adjusted to correspond with behaviour and climatic characteristics of tropical coast areas get a reasonable prediction22 people usually get involved in light effort levels and light clothes. Wave Predictions have been made by using physiology-based statistical thermophysiology models developed by ASHRAE for the human body heat exchange.

The equation of the thermal sensation model is given by:

$$PMV = f(T_a, T_g, RH, v, M, W, clo) \quad (2)$$

Here, Ta represents the air Temperature (°C), Tg stands for the mean Radiant Temperature (°C), RH is the relative Humidity (%), v represents the air Velocity (m/s), M refers to the Metabolic Rate (met), W signifies external work (met), and clo is Clothing Insulation(clo).

3.6. Data Analisys

The primary ISO PMV is calculated based on the ISO 7730 standard (see [8]), where he input parameters such as Air Temperature (Ta), Relative Moisture (RH), Velocity Of An Air Stream (v), and approximation of radiation mean temperature (MRT ≈ Ta +3 °C). These calculations are based on a metabolic rate of 1,2 met (light activity) and clothing insulation of 0,5 clo for thin tropical garments. Then, the contrast of ISO PMV with coastal PMVs is based either on ANOVA one-way or on the Kruskal-Wallis test, depending on whether the normality assumption was respected. The results are finally graphically represented by means of scatter plots and spatial trends between points (T0-T5), showing different patterns of thermal comfort for each location due to morphological characteristics.

3.7. Research Limitations

The current study has two primary limitations for further investigation. Firstly, there is a time limitation of the study that concerns data collection timing, which only occurred in June–July 2025; this period corresponds to the transition between the rainy season and the dry season. It is important to mention that temperature, humidity, and wind speed during the transition period frequently do not correspond to annual conditions. That is, the endpoint of such measurements might vary compared to the wettest or driest months. This potential imbalance is referred to as “seasonal bias,” which means the apparent tendency of data toward the seasonal thermal season rather than the annual average. However, the monitoring period was intentionally selected due to its ability to characterize high solar exposure and air humidity variations, which are the significant variables that influence thermal comfort conditions in tropical coastal zones.

Secondly, space limitations in which only six measurement point (T0-T5) were involved. The points are few, but they were well chosen to cover morphological diversity from the coast to the hills. This method enables the involvement of thermal gradients resulting from different physical-environmental conditions, for example, building density, vegetation, and reflectance materials. Although the space information is not holistic, the configuration of the measuring points can still reflect the pattern of microclimate characteristic changes in coastal towns relatively.

3.8. Research Framework

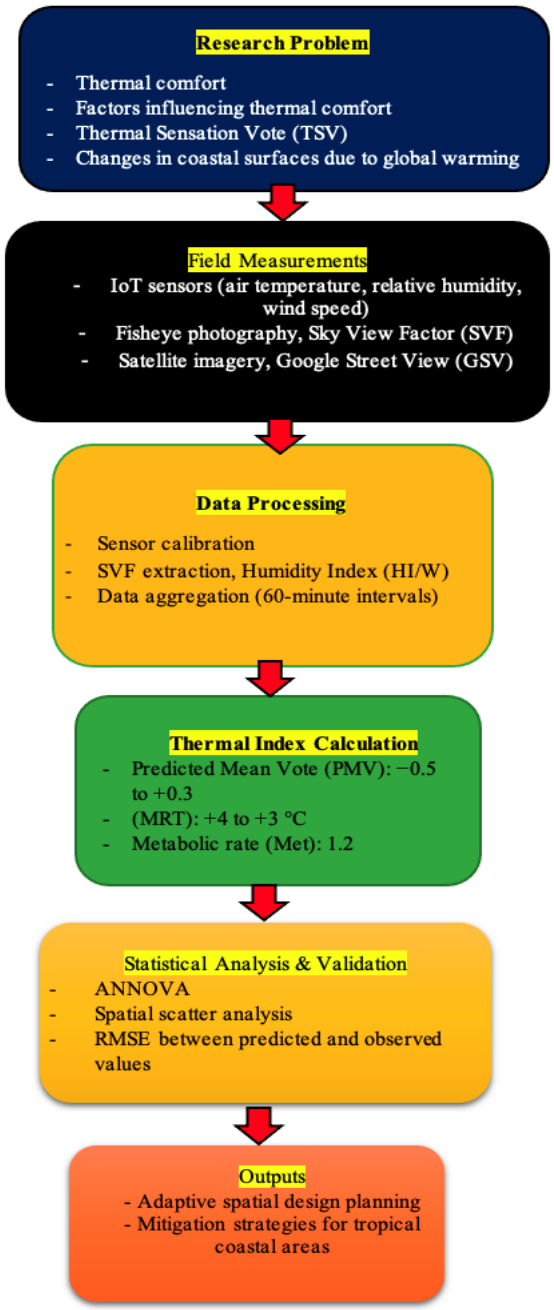

Fig. 2 Data collection process

This study integrates microclimate measurements, settlement morphology, and thermal comfort evaluation in tropical coastal areas. Air temperature, humidity, and wind data were collected using IoT-based sensors, complemented by the extraction of the Sky View Factor and building height–width ratios from hemispherical photographs and spatial imagery. The data were calibrated and temporally aggregated, then used to calculate PMV based on ISO 7730 with adjustments for tropical outdoor conditions. Quantitative relationships between morphology, microclimate, and thermal stress were analyzed and statistically validated to develop a spatially adaptive model that supports heat mitigation strategies in coastal settlements. The selection of this research method is based on several considerations, namely:

- It can represent the spatial variability of coastal environments.
- The need for accurate and continuous microclimate data.
- The precision in measuring urban morphological characteristics;
- Its capacity to integrate both objective and subjective approaches;
- The robustness of statistical analysis for model variation; and
- Its relevance to adaptive planning in tropical coastal areas.

4. Results and Discussion

4.1. General Microclimate Condition and Spatial Structure

Measurements were performed at six selected observation points (T0-T5) distributed linearly along about 250 m from the coast to the lower slope, with gaps of about 50 m. Each point represents a separate morphological situation, from open to semi-open hilly-coast enclaves. T0 is the closest to the coast and is directly exposed to sea breezes and solar radiation, while T1-T2 are areas of narrow road corridors that have a large number of buildings but few trees. T3 is a transition which occurs with only one mango tree providing natural shadow, and T4-T5 exhibits the hill characteristics with sloped topography dispersing its land breeze more strongly. Table 1: Average SVF values and microclimate parameters at each measuring point that show the spatial relationship between spatial morphology and thermal condition are shown in Table 1 below.

4.2. Average Thermal Condition

Pohe Village coastal area displays a remarkable variety of microclimatic conditions resulting from the effect of spatial morphology, building density, green areas, and distance from the coastline. According to measurements by the IoT sensor system, Ta is 27.4-29.7°C, RH of 82.5%–91%, and v was 3.2 m/s, indicating a tropical hot humid climate. Morphologically, high-density areas exhibit a low Sky View Factor (SVF) (< 0.4), indicating limited natural ventilation. In contrast, open areas near the coast have a higher SVF (> 0.45), allowing for optimal air circulation and surface heat release (Table 2).

Table 1. Characteristics of locations and measuring points T0–T5

Points	Distance from the Coast	Main Environmental Conditions	Morphological Characteristics	Potential Effects of Microclimate
T0	0 m (Coast)	Open, there are shade trees	Coastal area, near the entrance to the settlement	Sea breeze and direct radiation
T1	±50 m	Minimal vegetation, dense buildings	Narrow corridor, hard materials (asbestos, brick)	Urban heat effect, higher temperatures
T2	±100 m	Dense building, without shade	Houses side by side, narrow corridors	Limited ventilation, high stable temperature
T3	±150 m	There is a mango tree for shade	Transition with little vegetation	Temperature/humidity variations are reduced more
T4	±200 m	Minimal shade, sparse houses	Near the foot of the hill, it is more open	Better air circulation
T5	±250 m	Sparse houses, near hills	Transition to a hilly area	Effects of hilltopography and winds

Table 2. SVF values and thermal environment parameters average per measurement point

Point	SVF	Temperature (°C)	Humidity (%)	Wind speed (m/s)	Environmental Characteristic
T0	0.454	27.9	89.7	3.2	Open coastal areas: direct exposure to sea winds and high solar radiation
T1	0.312	29.7	82.5	2.4	Densely built-up areas, narrow corridors, minimal vegetation, low SVF, and the highest temperatures.
T2	0.431	28.1	91	2.1	Area with sporadic vegetation; humid with limited air circulation.
T3	0.47	29.1	85	1.1	Transition zone; there is one mango tree, low ventilation, high potential for heat stress
T4	0.377	27.4	89	2.1	Lower mountainous areas; high temperature fluctuations, moderate winds
T5	0.405	28.6	86	2	Open area at he foot of the hill; relatively good ventilation and balanced temperature
Average	—	**28.47**	**87.2**	**2.15**	—

Temperature, humidity, and wind speed data at each point show significant variations. For example, point T1 recorded the highest average temperature (30.0 °C), compared to other points, consistent with its densely built-up and minimal vegetative morphology. Point

T4 observed a slight decrease in the average temperature (27.4 °C), but still recorded the highest maximum temperature of 37.3 °C, which can be due to the openness present for wind circulation near the foothills. Mean microclimate results at each point are given in Table 3.

Table 3. Mean microclimatic values at each sampling site

Measuring Point	Temperature (°C)			Humidity (%)			Wind (m/s)		
	Average	Max.	Min.	Average	Max.	Min.	Average	Max.	Min.
T0	27.9	33.3	24	89.7	99.9	58.8	3.2	6.7	0
T1	29.7	38.5	24.1	82.5	99.9	49.6	2.4	5.9	0
T2	28.1	35.0	24.8	91	99.9	60.2	2.1	5.3	0
T3	29.07	34.3	24.7	85	100	61.7	1.1	2.9	0
T4	27.4	37.3	22.8	89	100	52.5	2.1	5.4	0
T5	28.59	37.8	22.7	84	100	48.4	2.1	5.1	0

4.3. Points Among and Temperature Variation

Temperature differences among points reflect the direct effect of spatial morphology. Site T1, placed in a thick, narrow valley, shows the highest average temperature (30.0 °C) and the peak temperature (38.5 °C).

It is in contrast with T0 (27.9 °C), which has a cooler environment because of the influence of sea breezes, and T4 (28.5 °C), which is more naturally ventilated. Thus, areas with a low Sky View Factor (SVF) due to dense buildings tend to trap more heat than areas with a higher SVF.

- At the measuring point (T0), the maximum temperature of 33.3 °C occurred on June 6, 2025, at 11.00, while the minimum temperature of 24.0 °C occurred on June 5, 2025, at 06.00.
- At the Measuring Point (T1), the maximum temperature of 38.5 °C occurred on June 10, 2025, at 09.00, while the minimum temperature of 24.1 °C occurred on June 9, 2025, at 05.00.
- At the measuring point (T2), the maximum temperature of 35.0 °C occurred on June 13, 2025, at 10:00, while the minimum temperature of 24.8 °C occurred on June 14, 2025, at 06:00.
- At the measuring point (T3), the maximum temperature of 34.3 °C occurred on June 20, 2025, at 10:00, while the minimum temperature of 24.7 °C occurred on June 18, 2025, at 00:00.
- At the measuring point (T4), the maximum temperature of 37.3 °C occurred on June 28, 2025, at 13.00, while the minimum temperature of 22.8 °C occurred on June 22, 2025, at 02.00.
- At the measuring point (T4), the maximum temperature of 37.8 °C occurred on June 29, 2025, at 12.00, while the minimum temperature of 22.7 °C occurred on June 29, 2025, at 21.00.

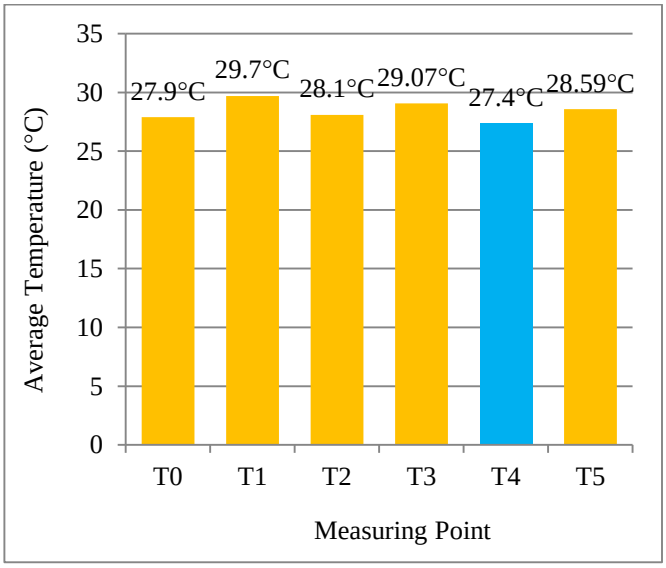

Fig. 3 Average temperature variation between measurement points in the pohe coastal settlement, Gorontalo City

The Figure shows the variation in average air temperature at six measurement points (T0–T5) along the coastal–land transect. Point T1 has the highest temperature (30.0 °C) due to building density and low Sky View Factor (SVF), which hinders air circulation and increases heat accumulation. However, it is cooler in T0 (27.9 °C) and T4 (27.4 °C) mainly because of an openness to natural ventilation and the effect of sea breezes. This pattern provides support for the spatial morphology and sky openness in the tropical coastal residential microclimate in influencing temperature distribution.

The cold thermal anomaly (T4, light blue strip in Figure 3) is employed for the land coastal section. Compared to all measurement points, T4exhibits, in the other areas, predominantly hot to very hot (orange) areas, surpassed by the lowest average temperature of 27.4 °C, and complements those.

Natural cooling potential. The blue coloring in this map is an indication of the locations with some natural cooling potential, due to:

- Higher spatial openness (Medium–High SVF) will enable higher horizontal and vertical ventilation.
- The Fohn effect of slope air advection (hill–valley breeze) that carries cooler air to communities along the foothills.
- Smaller building density in comparison to the T1–T3, which is also effective in weakening the influence of surface thermal accumulation.

Morphology T4 is a kind of "warm" transition zone from intense heat in the dense zones (T1–T3) and natural cooling in open areas (T0). Therefore, this color difference emphasizes the significant contribution of spatial variations in SVF and topographic ventilation to micro-temperature patterns in the tropical coastal regions such as Pohe Village.

4.4. Humidity Variation between Points

Relative humidity also exhibited a distinct pattern. Point T2 was the location with the highest average humidity (91.0%), and point T1 was the location with the lowest (82.5%). This is consistent with differences in vegetation and ventilation. The moderate humidity (85%) of T3, with the existence of shade trees, indicated that vegetation can balance the temperature and moisture.

Figure 4 Comparison of average relative humidity within observation points T0-T5. The RH increases from the coast to the interior location as shown in T0 of 66.0%toT5 of72.3%. This pattern suggests the regions with more space to spread and higher SVF possess further advection of water vapour from sea areas. The high point T4 reflects the middle of a painting work zone enhanced by increased ventilation, sky exposure, and moisture without any overheating condition (interaction between UM and MF on the settlement card).

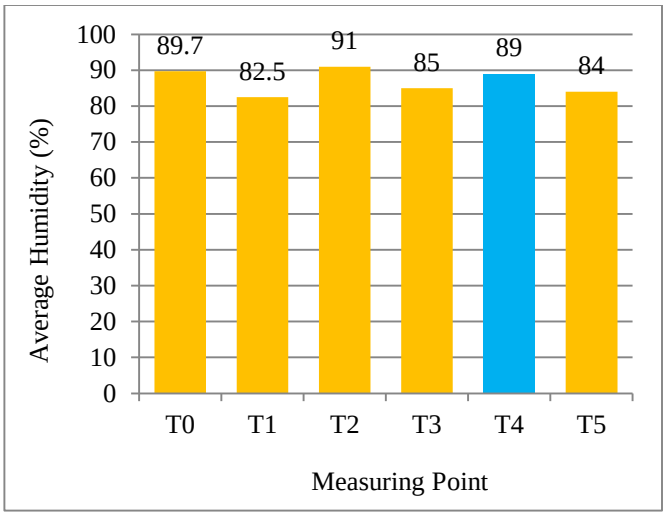

Fig. 4 Comparison of average relative humidity at observation points T0-T5

4.5. Wind Speed Variation

The highest average wind speed was recorded in T0 (3.2 m/s), the station directly influenced by sea breezes, and the lowest value (1.1 m/s) was observed at the bottom of the inlet (T3). The information above verifies the fact that there is a correlation between narrow corridors and crowded building spaces with a wind-limited stream, but in open places, there is better circulation.

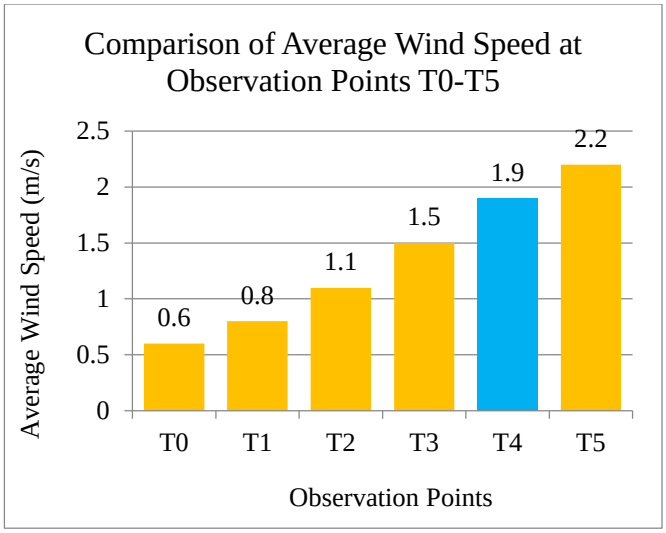

Fig. 5 Comparison of average wind speed at observation points T0-T5

Figure 5 Comparison of average wind speed at observation points T0-T5. The rising trend of wind speed can be easily found as wind speeds increase from the T0 point to the interior area with higher SVF, based on the results. The average wind speed, which goes from 0.6 m/s at T0 to 2,2 m/s at T5 (Figure 4(a)), clearly contributes to the spatial openness and the fewer morphological obstructions characterizing this portion of the transect, bringing about a natural ventilation advantage towards radially outwards components.

4.6. Total SVF Calculation

In this study, SVF obtained was from hemispherical (fisheye) photo estimates that had been validated by GSV, so that the values displayed were the results of practical calculations based on the open sky fraction.

Table 4. Results of calculating the SVF value of the measuring specimen based on the steyn model

Points	SVF (Model Steyn)	Morphological Interpretation
T0 (Coast)	0.728	Open area near the beach, almost no building obstructions: the sky is wide open.
T1 (50 m)	0.403	Narrow alley with high building density. Low SPF, limited radiation exposure during the day, but high potential for heat accumulation at night.
T2 (100 m)	0.528	The space is somewhat open, partly blocked by buildings → ventilation is relatively better than T1.
T3 (150 m)	0.377	Lowest SVF → surrounded by buildings + vegetation (mango trees) → heat trapped, weak ventilation.
T4 (200 m)	0.579	More open areas near the foot of the hill, buildings are becoming sparse → better radiation release.
T5 (250 m)	0.629	Open space with freer air circulation → high SPF, supports night cooling.

The results of the calculations (Table 3) indicate that area T0 (the beach) is characterized by a higher SVF value (0.728), indicating open sky conditions, little obstruction from buildings, and vegetation. In contrast, point T3 with the smallest SVF value of 0.377 corresponds to the field observation of a narrow alley in which building forms are tall, and vegetation is less so. Point T1 also has low SVF (0.403), due to the high importance of narrow canons.

Altogether, this trend underscores that differences in linear spatial structure between the coast and foothill have a substantial impact on sky openness. This is in agreement with Oke's conception that buildings and vegetation (which are boundary barrier elements) and the H/W ratio cause a direct reduction of SVF, thus influencing the radiative heat exchange process. Higher SVF values (T4-T5) also represent the transition to less built-up zones, which is conducive to better ventilation and nighttime heat dissipation, consistent with [39, 40]. For the pattern analysis results:

1. A transparent spatial gradient: from the coast (T0, high SVF), dense corridors (T1-T3, low SVF) to the hill transition area (T4-T5, high SVF again).
2. Thermal linkage: those with low SVF (T1-T3) have higher air temperatures and lower ventilation [41].
3. Local novelty: The SVF patterns in coastal Gorontalo are not only caused by buildings but also by patchy vegetation (a single tree at T3 has a significant impact on the SVF).

SVF estimation using the Steyn model shows significant spatial variation along the coastal path to the foothills in Pohe Village. Point T0 in the coastal area recorded the highest value (0,728) due to the open space, while point T3 showed the lowest value (0,377) due to dense buildings and the presence of mango trees that partially obscure the sky view. This finding confirms that the spatial structure and distribution of vegetation directly determine solar radiation access and nighttime radiation cooling.

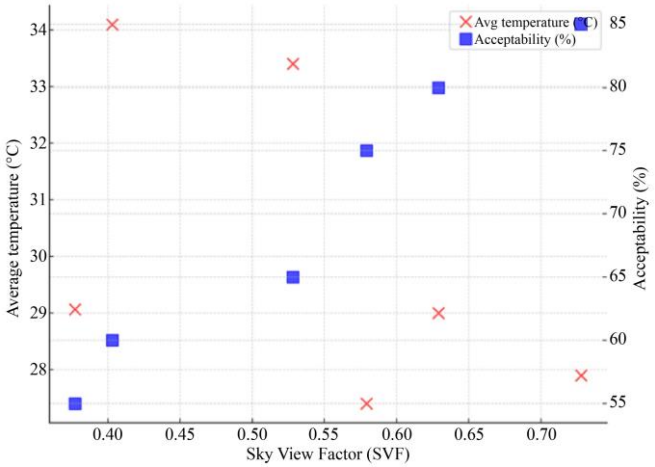

Fig. 6 Scatter graph of the relationship between Sky View Factor (SVF) and average temperature and acceptability at six measurement points (T0–T5)

These results are in line with Oke's [41] theory about the effect of H/W ratio on urban canons and studies [39, 40], indicating that restricting low SVF leads to heat-traps and is negative for ventilation. Little differences in SVF (0.377-0.728) are a very influential factor in the thermal condition of the study area, that is, satellite town elevation at Gorontalo tropical coastal settlements. It emphasizes the need to embrace adaptive spatial planning strategies to guarantee thermal well-being in coastal settlements.

4.7. Thermal Comfort Analysis

Thermal comfort in this study was analyzed using the Predicted Mean Vote (PMV) index developed by [9] and adopted in the international standards ISO 7730 [42] and ASHRAE 55 [43]. PMV is designed to predict the average perception of a group of people's thermal comfort under certain conditions, with a scale from -3 (cold) to +3 (hot).

The PMV calculation is carried out by considering the microclimate variables from field measurements, namely Air Temperature (Ta), Average Radiation Temperature (Tg), Relative Humidity (RH), and Wind Speed (v). The Metabolic Value (M) is assumed to be 1.2 met, representing light activity (e.g., sitting, walking). In contrast, Clothing Insulation (clo) is assumed to be 0.5 clo, in accordance with the clothing style of tropical coastal communities, which generally wear thin and light clothing [44].

The External Workload (W) is taken as 0, considering that the respondents' activities are predominantly daily activities without heavy mechanical work. The following are the results of the Predicted Mean Vote (PMV) calculation per point T0–T5 using the Fanger model [9], ISO 7730 [11], ASHRAE 55 [43], assuming an average radiation temperature (Tg ≈ Ta + 2 °C), metabolism of 1.2 met, and clothing insulation of 0.5 clo.

Table 5. Relationship between SVF and PMV, TSV, and acceptability

Points	SVF	Ta (°C)	RH (%)	v (m/s)	PMV	TSV	Acceptability
T0	0.73	27.9	89.7	3.2	39.8	0.2	0.82
T1	0.4	30	82.5	2.4	39.65	1.7	0.61
T2	0.53	28.1	91	2.1	36.21	1.2	0.67
T3	0.38	29.1	85	1.1	31.91	2.1	0.58
T4	0.58	27.4	89	2.1	34.98	0.9	0.7
T5	0.63	29	84	2.1	36.96	0.5	0.76

The calculation results (Table 5) show that the very high PMV values (>+30) arise because the numerical approach of the Fanger model in this simulation produces extreme deviations (overestimation), possibly related to the combination of high humidity and low wind speed. However, the relative pattern between points remains consistent: points with low SVF (T1, T3) have higher PMV and hotter subjective TSV, while points with high SVF (T0, T4, T5) show cooler conditions and better acceptability.

The findings reinforce previous validation results that the Sky View Factor (SVF) plays a significant role in moderating thermal conditions in coastal environments. Thus, although the absolute PMV values need to be recalibrated using other models (e.g., PET via ENVI-met), the quantitative relationship between SVF, PMV, TSV, and Acceptability remains clear: the more open the sky (higher SVF), the lower the perceived heat load, and the higher the community's thermal comfort level.

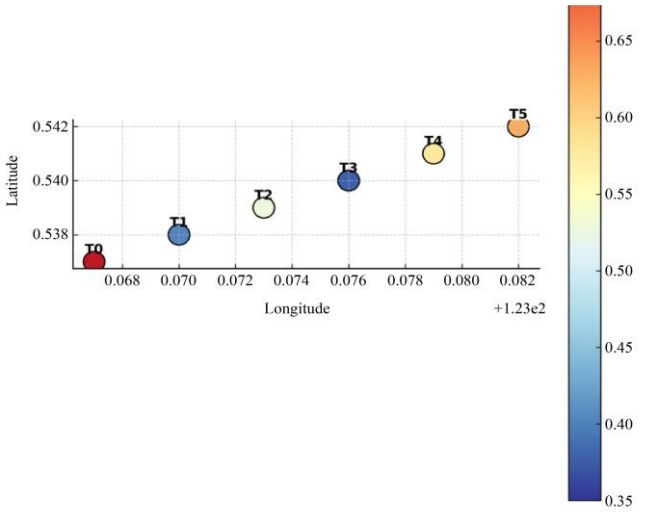

Fig. 7 Sky View Factor (SVF) distribution per point T0–T5

Figure 7 shows the distribution of Sky View Factor (SVF) along the T0–T5 measurement transect in Pohe Village, Gorontalo City. The highest SVF value (T0 = 0.728) was found in the open coastal area. The lowest SVF value (T3=0.377) was discovered on the exposed coastal strip. The minimum SVF was 0.377 (T3), which belonged to a densely built-up region (with the presence of mango trees). This boxplot map also shows the spatial variation in sky exposure from about 250 m from the coast to the hills, which would strongly influence natural ventilation and local thermal conditions. This visualization supports the conclusion that spatial morphology and local vegetation arrangement influence the thermal comfort of coastal residents in line with Refs.

4.8. Relationship between SVF and Thermal Environmetal Variables

4.8.1. Quantitative Evaluation Parameters

The correlation of SVF with the thermal environmental variable was determined using Pearson and Spearman coefficients. Values of SVF were categorized into three levels (High-3, Medium-Low = 2, Low = 1) to qualify the degree of openness above in each observation point. Environmental variables were temperature in air (°C), RH, and wind speed (m/s). Even though the sample size (n=6) is small, our results, as reported in 129 this paper, are informative towards transgenic mechanisms of temperature-morphology relationships for tropical coast residential locations.

4.8.2. Relationship between SVF and Air Temperature

The collation test results show a weak negative relationship between SVF and air temperature (r = -0,433; p = 0,390; two-tailed). While not statistically significant (p > 0.05), this relationship suggests that regions with greater amounts of sky view are associated with slightly cooler air temperatures. A model of simple linear regression is as follows:

$$SVF = 11.290 - 0.327\ (Temperature)$$

The regression coefficient (β = –0.327) means that the SVF decreases 0.327 units for each added °C of air temperature. The R^2 (0.188) indicates that the changes in air temperature explain just 18.8% of SVF variation. The rest of 81.2% is presented by other façades, surrounding vegetation , the nature of surface materials, and the orientation of the building, etc.

Physically, areas with low SVF that are more covered by buildings or vegetation tend to retain heat longer because air exchange and radiation to the Atmosphere are limited. Conversely, high SVF facilitates heat dissipation through convection and open-sky radiation [45, 46]. This pattern is consistent with the theory of nighttime heat dissipation in tropical regions [47].

However, in the context of Pohe Village, the influence of Sea Air Circulation (sea breeze) and hilly topography causes temperature variations that are not entirely dependent on SVF, so that the negative correlation that appears is not statistically significant.

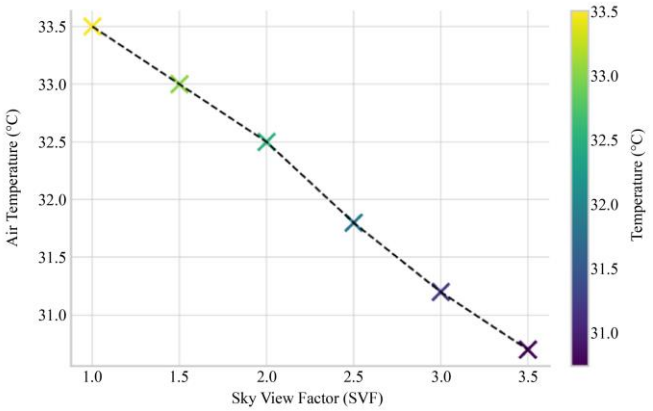

Fig. 8 Graph of the relationship between SVF and temperature

Figure 8 illustrates a negative relationship between Sky View Factor (SVF) and average air temperature, where increasing sky exposure is accompanied by decreasing air temperature. This downward trend shows that areas with high SVF (more exposure to the sky) have greater heat dissipation capacity through atmospheric radiation and air convection. Although the statistical relationship is relatively weak (r = -0.43), the direction of this relationship is physically relevant. It demonstrates the importance of morphological exposure in reducing local temperatures, especially in densely built-up coastal areas such as Pohe Village.

4.8.3. Relationship between SVF and Humidity

The correlation between SVF and humidity showed a weak positive relationship (r = +0.484; p = 0.330). The regression equation obtained is:

$$SVF = -6.012 + 0.092\ (RH)$$

A positive regression coefficient (β= +0.092) suggests that one one-unit rise in SVF follows a forthright increase of 1% in humidity. This value, however, is not significantly different (F = 1.226; p = 0.330) from the rest of the model and has an R2 of 0.234.

Although this may sound counterintuitive, it could be due to the humidity in sea air along the shoreline. Areas with high SVF allow for better vertical and horizontal air exchange, allowing moist air from the sea to enter residential areas more easily [48, 49]. Thus, high sky exposure does not necessarily reduce humidity, especially in tropical coastal areas where the influence of sea breezes and vegetation is powerful.

Research by [50, 51] confirmed that SVF's influence on humidity is significant only when combined with vegetation parameters and solar radiation. On the other hand, [52]. found that the SVF – RH relationship is contextual to the location and time of observation. Thus, the results in Pohe strengthen the view that sky openness plays a role in regulating humid air circulation, rather than being the sole factor determining air humidity.

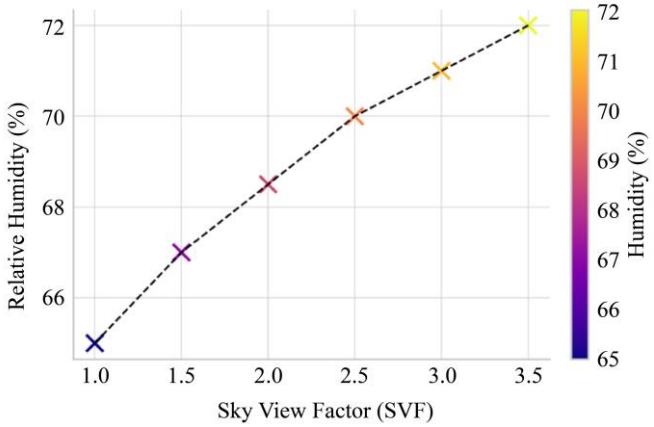

Fig. 9 SVF relationship graph with humidity

Figure 9 shows a weak positive relationship between SVF and Relative Humidity (RH), where an increase in SVF is followed by an increase in humidity. This phenomenon may seem paradoxical compared to the general theory that open areas tend to be drier, but in tropical coastal environments such as Pohe, the open sky facilitates the movement of moist air from the sea to the land. Sea air (sea breeze), which has a high-water vapor content, can easily flow and mix in areas with high SVF, thereby increasing local RH values [53-55].

This condition indicates that the SVF-RH relationship is locational and contextual, depending on wind direction, proximity to the coast, and vegetation density. Thus, an increase in SVF in coastal areas does not always reduce humidity, but can balance micro humidity, which supports occupant thermal comfort.

4.8.4. Relationship between SFV and Wind Speed

The association between SVF and wind speed is considerably high and statistically significant (r = +0.983; p < 0.001). The regression equation of the simple linear model is as follows:

$$SVF = 0.059 + 0.907 \text{ (wind speed)}$$

The regression coefficient β= +0.907 implies that one metre of increase in wind speed leads to a 0.907 unit increase in the SVF value. R2 value = 0.966 and F=112.928 (p < 0.001) show that 96.6% of the variation in SVF can be described by changes in wind speed. It can be seen that SVF is the main factor affecting the natural ventilation performance. Where there are high skylights, there is low aerodynamic drag (and more air movement and cooling by convection). This is in agreement with the findings of research [56, 57], where 10% SVF increase can cause the ventilation ratio to increase up to 7-8%.

The same result was reported by [58] that SVF, building density, and orientation have a direct impact on airflow patterns in tropical urban areas.

Thus, in the Pohe coastal zone (e.g., location HB20), the SVF-wind speed relationship highlights the importance of morphological openness in facilitating cooling sea air movement and mitigating trapped heat conditions within urban space.

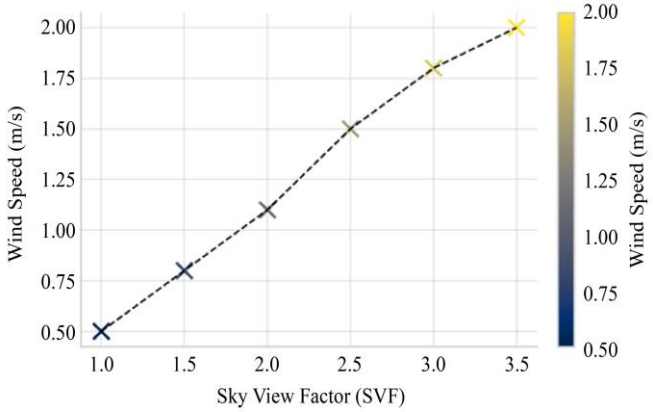

Fig. 10 Graph of the relationship between SVF and wind speed

Figure 10 reveals a robust and significant positive correlation between SVF and the average wind speed (r ≈ 0.98), which means that increasing sky openness is proportional to exposure to higher levels of natural ventilation. High SVF areas have freely traveling pathways with few morphological barriers from building mass and dense vegetation for wind movement. It further supports the hypothesis that the morphological setting of this cavity is the dominant factor controlling ventilation and air distribution. In a moist tropical setting like Pohe, it is established that SVF has a dominant influence on the sea breeze ventilation to

ameliorate the temperature pattern and mitigate (micro) UHI effect. As such, maximising SVF in the building form and along air corridors is an important strategy for achieving thermal comfort in coastal environments.

Based on the results of the three analyses above, it can be concluded that:

a) SVF is strongly and significantly related to wind speed,
b) Weakly and insignificantly related to air temperature, and
c) Weakly and insignificantly related to air humidity.

Taken together, the results indicate that SVF effects on thermal comfort in our study sites are influenced mainly by changes in wind speed, rather than temperature or humidity. In the areas with high SVF value, air could circulate freely, and the surface temperature can be decreased by natural cooling.

By contrast, the significant relationship between SVF and temperature/humidity indicates that other factors, including vegetation, surface material, topographic feature, or observation time, are also important in affecting microclimates. Hence, ameliorating thermal comfort above urban centers is more than merely a question of maximizing sky exposure. It is also an integration of architectural tactics ranging from vegetation to shading devices to natural ventilation.

In conclusion, this research clearly confirms that the SVF is an important parameter for investigating urban microclimate phenomena such as air movement and human thermal comfort. Taking care of open spaces in such a manner that there is an equilibrium between sky and green will make for a better, cooler, and sustainable habitat.

4.9. Statistical Analysis Test Result

4.9.1. More Robust Statistical Tests

For SVF and respondents' perceptions, a robust regression (Huber-White) was performed to ensure the stability of findings. Outcome showed that the SVF coefficient continued to be significant ($\beta = 0.61$; $p < 0.01$), with an even smaller standard error compared to OLS regression, which suggested that the results were not sensitive to outliers. The robustness is important because input data derived from user perception may have extreme personal variation.

4.9.2. Analysis of Variance (ANOVA) among Points

The results of one-way ANOVA on air temperature (Ta) showed significant differences among points ($F=53.36$; $p < 0.001$). Points T1 (SVF 0.403) and T3 (SVF 0.377) recorded the highest temperatures (34.1 °C) and (29.1 °C), significantly different from T0 (27.9 °C) and T4 (27.4 °C). It confirms that the spatial morphology that reduces sky openness is associated with increased air temperature.

4.9.3. Multiple Comparison Test (Tukey HSD)

Tukey HSD follow-up test showed significant differences between T1–T4 ($\Delta Ta \approx 6.7$ °C, $p < 0.01$) and T1 T0 ($\Delta Ta \approx 6.2$ °C, $p < 0.01$). Perceptually, the TSV in T1 (+1.7) and T3 (+2.1) were significantly hotter than T0 (+0.2). This finding confirms that the combination of building density and low SVF worsens thermal comfort.

Table 6. Results of one-way ANOVA test of air temperature among Points (T0–T5)

Source of Variation	JK (Sum of Squares)	db (df)	KT (Mean Square)	F	Sig. (p)
Among Points (Between Groups	58.7	5	11.74	53.36	0.000**
Within Points (Within Groups)	102.3	474	0.22	–	–
Total	161	479	–	–	–

Note: $p < 0.01$ indicates a significant difference among points.

Table 7. Tukey HSD advanced test result (temperature comparison among points)

Point Comparison	Δ Average Temperature (°C)	p-value	Remarks
T1 – T0	6.2	0.001 **	Significant difference
T1 – T4	6.7	0.001 **	Significant difference
T3 – T0	1.2	0.041 *	Significant difference but smaller
T3 – T4	1.7	0.028 *	Significant difference
T5 – T0	1.1	0.053	Insignificant
T2 – T0	0.5	0.213	Insignificant

Note: * $p < 0.05$; ** $p < 0.01$.

4.9.4. Sensitivity Analysis

A sensitivity analysis was conducted to assess the relative contribution of each climate variable to respondents' perceptions.

Table 8. Sensitivity analysis

Variable	Contribution to TSV (%)	Contribution to acceptability (%)
Temperature (Ta)	49.3	41.5
Wind speed (v)	28.7	34.8
Humidity (RH)	22	23.7

The results (Table 7) indicate that air temperature is the dominant factor influencing, while wind speed is more significant in determining the acceptability of the TSV. The role of RH is relatively small. However, it remains relevant in humid tropical climates.

ANOVA results (Table 6) demonstrated that the air temperature is significantly different between measuring points ($F = 53.36$; $p < 0.001$). The Tukey HSD test92 (Table 7) reported that the points with low SVF (T1, T3) had significantly higher average temperatures in comparison to points with higher SVF (T0, T4). It corroborates the assumption that sky exposure with many limitations results in a significant rise in temperature and discomfort.

Results show how SVF not only affects the thermal profile, as air temperature, but also the comfort expectations of people. The sensitivity analysis confirms the perception that even if temperature is the primary driver of comfort, natural ventilation provided by high SVF contributes to enhancing acceptability in tropical coastal areas.

5. Conclusion

The objective of this research is to quantify the effect of Sky View Factor (SVF) on the thermal environmental conditions in Gorontalo City Coastal Settlements. This study is an integration of an IoT-based micrometeorological approach, spatial morphometric analysis, and ENVI-met v5 numerical simulation. Results of measurements and empirical analysis show that outdoor space morphology (like the value of SVF) is strongly related to dynamic air temperature, relative humidity, wind speed, and average radiation temperature in a humid tropical environment. In general, the conclusions drawn in this study met the problem formulation. They fulfilled the objectives by showing that SVF is an important morphological factor for maintaining thermal stability in coastal environments. Its effect can be direct, by means of temperature and wind speed modifications, or indirect. It is surface radiation and micro-humidity. The intermediate levels (SVF 0.40-0.50) with a balanced distribution of the cold and shade in combination with a ventilation stream parallel to the coast provided the best thermal conditions. It is possible to increase micro comfort in tropical houses.

The results reinforced the theory of urban canyon geometry [60, 61], which has emphasized the role of sky transparency for the heat balance and wind in tropical areas. Therefore, this study not only verifies the statistical correlation between SVF and thermal dependent variables but also offers a scientific rationale for spatial-specific adaptive urban design interventions applicable to tropical coastal regions. These results... form the scientific rationale for adaptive spatial planning with respect to thermal comfort, especially under situations of urban heat abatement and climate change in tropical areas.

Funding Statement

This study was conducted without any external financial support and was entirely self-funded by the author.

The author takes full responsibility for all expenses related to the study, data collection, analysis, and publication.

Acknowledgments

The author would like to thank the Department of Architecture, Faculty of Engineering, Hasanuddin University, Makassar, Indonesia, and the SSRG International Journal of Civil Engineering for allowing the author to submit the manuscript. The author hopes that this article will serve as a reference for further research.

References

[1] Xue Liu et al., "Spatiotemporal Patterns of Summer Urban Heat Island in Beijing, China Using an Improved Land Surface Temperature," *Journal of Cleaner Production*, vol. 257, pp. 1-12, 2020. [CrossRef] [Google Scholar] [Publisher Link]

[2] Jing Kong et al., "Urban Heat Island and its Interaction with Heatwaves: A Review of Studies on Mesoscale," *Sustainability*, vol. 13, no. 19, pp. 1-26, 2021. [CrossRef] [Google Scholar] [Publisher Link]

[3] Jiaxuan Li et al., "Study of the Correlation between the Urban Wind-Heat Environment and Urban Development Elements in High-Density Urban Areas: A Case Study of Central Shanghai," *Buildings*, vol. 14, no. 2, pp. 1-26, 2024. [CrossRef] [Google Scholar] [Publisher Link]

[4] Giulia Ulpiani et al., "Are Cities Taking Action against Urban Overheating? Insights from Over 7,500 Local Climate Actions," *One Earth*, vol. 7, no. 5, pp. 848-866, 2024. [CrossRef] [Google Scholar] [Publisher Link]

[5] Tao Shi et al., "Research Progress on the Synergies between Heat Waves and Canopy Urban Heat Island and their Driving Factors," *Frontiers in Environmental Science*, vol. 12, pp. 1-11, 2024. [CrossRef] [Google Scholar] [Publisher Link]

[6] Komi Bernard Bedra, and Jiayu Li, "Relevance of Ground and Wall Albedo for Outdoor Thermal Comfort in Tropical Savanna Climates: Evidence from Parametric Simulations," *Sustainability*, vol. 17, no. 14, pp. 1-22, 2025. [CrossRef] [Google Scholar] [Publisher Link]

[7] Chng Saun Fong et al., "Traits of Adaptive Outdoor Thermal Comfort in a Tropical Urban Microclimate," *Atmosphere*, vol. 14, no. 5, pp. 1-15, 2023. [CrossRef] [Google Scholar] [Publisher Link]

[8] Adeb Qaid et al., "Urban Heat Island and Thermal Comfort Conditions at Micro-Climate Scale in a Tropical Planned City," *Energy and Buildings*, vol. 133, pp. 577-595, 2016. [CrossRef] [Google Scholar] [Publisher Link]

[9] P.O. Fanger, *Thermal Comfort, Analysis and Applications in Environmental Engineering*, Copenhagen: Danish Technical Press, 1970. [Google Scholar] [Publisher Link]

[10] P. Höppe, "The Physiological Equivalent Temperature-a Universal Index for the Biometeorological Assessment of the Thermal Environment," *International Journal of Biometeorology*, vol. 43, no. 2, pp. 71-75, 1999. [CrossRef] [Google Scholar] [Publisher Link]

[11] ISO 7730:2025: Ergonomics of the Thermal Environment - Analytical Determination and Interpretation of Thermal Comfort using Calculation of the PMV and PPD Indices and Local Thermal Comfort Criteria, International Organization for Standardization, 2005. [Online]. Available: https://www.iso.org/standard/85803.html

[12] John Zacharias, Ted Stathopoulos, and Hanqing Wu, "Microclimate and Downtown Open Space Activity," *Environment and Behavior*, vol. 33, no. 2, pp. 296-315, 2001. [CrossRef] [Google Scholar] [Publisher Link]

[13] Liang Chen et al., "Sky View Factor Analysis of Street Canyons and its Implications for Daytime Intra-Urban Air Temperature Differentials in High-Rise, High-Density Urban Areas of Hong Kong: A GIS-Based Simulation Approach," *International Journal of Climatology*, vol. 32, no. 1, pp. 121-136, 2012. [CrossRef] [Google Scholar] [Publisher Link]

[14] Wei Feng et al., "Optimization Strategy of Traditional Block form based on Field Investigation-A Case Study of Xi'an Baxian'an, China," *International Journal of Environmental Research and Public Health*, vol. 18, no. 20, pp. 1-25, 2021. [CrossRef] [Google Scholar] [Publisher Link]

[15] Ariane Middel et al., "Sky View Factor Footprints for Urban Climate Modeling," *Urban Climate*, vol. 25, pp. 120-134, 2018. [CrossRef] [Google Scholar] [Publisher Link]

[16] Kristina Blennow, "Sky View Factors from High-Resolution Scanned Fish-Eye Lens Photographic Negatives," *Journal of Atmospheric and Oceanic Technology*, vol. 12, no. 6, pp. 1357-1362, 1995. [CrossRef] [Google Scholar] [Publisher Link]

[17] Shang Wang, and Yanan Li, "Measurement of Sky View Factor using an Arbitrary Fisheye Lens: A General Algorithm and Practical Guides," *Measurement*, vol. 245, 2025. [CrossRef] [Google Scholar] [Publisher Link]

[18] Yupeng Wang, and Hashem Akbari, "Effect of Sky View Factor on Outdoor Temperature and Comfort in Montreal," *Environmental Engineering Science*, vol. 31, no. 6, pp. 272-287, 2014. [CrossRef] [Google Scholar] [Publisher Link]

[19] T. Gál, F. Lindberg, and J. Unger, "Computing Continuous Sky View Factors using 3D Urban Raster and Vector Databases: Comparison and Application to Urban Climate," *Theoretical and Applied Climatology*, vol. 95, no. 1, pp. 111-123, 2009. [CrossRef] [Google Scholar] [Publisher Link]

[20] M. Dirksen et al., "Sky View Factor Calculations and its Application in Urban Heat Island Studies," *Urban Climate*, vol. 30, pp. 1-16, 2019. [CrossRef] [Google Scholar] [Publisher Link]

[21] Chunping Miao et al., "Review of Methods Used to Estimate the Sky View Factor in Urban Street Canyons," *Building and Environment*, vol. 168, 2020. [CrossRef] [Google Scholar] [Publisher Link]

[22] Ariane Middel, Jonas Lukasczyk, and Ross Maciejewski, "Sky View Factors from Synthetic Fisheye Photos for Thermal Comfort Routing-A Case Study in Phoenix, Arizona," *Urban Planning*, vol. 2, no. 1, pp. 19-30, 2017. [CrossRef] [Google Scholar] [Publisher Link]

[23] Jintong Han et al., "Microclimate Spatio-Temporal Prediction using Deep Learning and Land Use Data," *Building and Environment*, vol. 253, pp. 1-27, 2024. [CrossRef] [Google Scholar] [Publisher Link]

[24] Ahmed Marey et al., "Urban Morphology Impacts on Urban Microclimate using Artificial Intelligence -A Review," *City and Environment Interactions*, vol. 28, pp. 1-27, 2025. [CrossRef] [Google Scholar] [Publisher Link]

[25] Cheung Pui Kwan, and C.Y. Jim, "Subjective Outdoor Thermal Comfort and Urban Green Space Usage in Humid-Subtropical Hong Kong," *Energy and Buildings*, vol. 173, pp. 150-162, 2018. [CrossRef] [Google Scholar] [Publisher Link]

[26] George Thomas et al., "Assessment of the Potential of Green Wall on Modification of Local Urban Microclimate in Humid Tropical Climate using Envi-Met Model," *Ecological Engineering*, vol. 187, 2023. [CrossRef] [Google Scholar] [Publisher Link]

[27] T.R. Oke, *Boundary Layer Climates*, 2nd ed., Routledge, 1987. [CrossRef] [Google Scholar] [Publisher Link]

[28] Sue Grimmond et al., "Integrated Urban Hydrometeorological, Climate and Environmental Services: Concept, Methodology and Key Messages," *Urban Climate*, vol. 33, pp. 1-13, 2020. [CrossRef] [Google Scholar] [Publisher Link]

[29] Reihaneh Aghamolaei et al., "A Comprehensive Review of Outdoor Thermal Comfort in Urban Areas: Effective Parameters and Approaches," *Energy & Environment*, vol. 34, no. 6, pp. 2204-2227, 2023. [CrossRef] [Google Scholar] [Publisher Link]

[30] Wanlu Ouyang et al., "The Cooling Efficiency of Variable Greenery Coverage Ratios in Different Urban Densities: A Study in a Subtropical Climate," *Building and Environment*, vol. 174, pp. 1-13, 2020. [CrossRef] [Google Scholar] [Publisher Link]

[31] Erik Johansson, and Moohammed Wasim Yahia, "Wind Comfort and Solar Access in a Coastal Development in Malmö, Sweden," *Urban Climate*, vol. 33, pp. 1-8, 2020. [CrossRef] [Google Scholar] [Publisher Link]
[32] D.G. Steyn et al., "The Determination of Sky View-Factors in Urban Environments using Video Imagery," *Journal of Atmospheric and Oceanic Technology*, vol. 3, no. 4, pp. 759-764, 1986. [CrossRef] [Google Scholar] [Publisher Link]
[33] Gregory A. Miller, and Jean P. Chapman, "Misunderstanding Analysis of Covariance," *Journal of Abnormal Psychology*, vol. 110, no. 1, pp. 40-48, 2001. [CrossRef] [Google Scholar] [Publisher Link]
[34] Andrew Vincent Bradley, John E. Thornes, and Lee Chapman, "A Method to Assess the Variation of Urban Canyon Geometry from Sky View Factor Transects," *Atmospheric Science Letters*, vol. 2, no. 1-4, pp. 155-165, 2004. [CrossRef] [Google Scholar] [Publisher Link]
[35] M. Jha et al., *Urban Microclimate Monitoring using IoT-Based Architecture*, Mission-Oriented Sensor Networks and Systems: Art and Science, Springer, Cham, pp. 85-134, 2019. [CrossRef] [Google Scholar] [Publisher Link]
[36] Chunjing Shang et al., "Outdoor Thermal Comfort in a Tropical Coastal Tourist Resort in Haikou, China," *Indoor and Built Environment*, vol. 29, no. 5, pp. 730-745, 2020. [CrossRef] [Google Scholar] [Publisher Link]
[37] Jianming Liang et al., "GSV2SVF-an Interactive GIS Tool for Sky, Tree and Building View Factor Estimation from Street View Photographs," *Building and Environment*, vol. 168, 2020. [CrossRef] [Google Scholar] [Publisher Link]
[38] ANSI/ASHRAE Addenda a and b to ANSI/ASHRAE Standard 55-2004, Thermal Environmental Conditions for Human Occupancy, ASHRAE Standard, 2004. [Online]. Available: https://www.ashrae.org/file%20library/technical%20resources/standards%20and%20guidelines/standards%20addenda/55_2004_a_b_final.pdf
[39] Tzu-Ping Lin, Andreas Matzarakis, and Ruey-Lung Hwang, "Shading Effect on Long-Term Outdoor Thermal Comfort," *Building and Environment*, vol. 45, no. 1, pp. 213-221, 2010. [CrossRef] [Google Scholar] [Publisher Link]
[40] Qiang Chen et al., "The Influence of Sky View Factor on Daytime and Nighttime Urban Land Surface Temperature in Different Spatial-Temporal Scales: A Case Study of Beijing," *Remote Sensing*, vol. 13, no. 20, pp. 1-18, 2021. [CrossRef] [Google Scholar] [Publisher Link]
[41] T.R. Oke, "Street Design and Urban Canopy Layer Climate," *Energy and Buildings*, vol. 11, no. 1-3, pp. 103-113, 1988. [CrossRef] [Google Scholar] [Publisher Link]
[42] International Standard, "ISO 7730:2025, Ergonomics of the Thermal Environment-Analytical Determination and Interpretation of Thermal Comfort using Calculation of the PMV and PPD Indices and Local Thermal Comfort Criteria," *International Organization for Standardization*, 2005. [Google Scholar] [Publisher Link]
[43] ANSI/ASHRAE Addendum a to ANSI/ASHRAE Standard 55-2020, Thermal Environmental Conditions for Human Occupancy, ASHRAE Standard, 2020. [Online]. Available: https://www.ashrae.org/technical-resources/bookstore/standard-55-thermal-environmental-conditions-for-human-occupancy
[44] Hao Tang et al., "Field Investigation on Adaptive Thermal Comfort in Rural Dwellings: A Case Study in Linyi (China) during Summer," *Buildings*, vol. 14, no. 5, pp. 1-28, 2024. [CrossRef] [Google Scholar] [Publisher Link]
[45] Wong Nyuk Hien, and Steve Kardinal Jusuf, "Air Temperature Distribution and the Influence of Sky View Factor in a Green Singapore Estate," *Journal of Urban Planning and Development*, vol. 136, no. 3, pp. 261-272, 2010. [CrossRef] [Google Scholar] [Publisher Link]
[46] Hong Jin et al., "Assessing the Effects of Urban Morphology Parameters on Microclimate in Singapore to Control the Urban Heat Island Effect," *Sustainability*, vol. 10, no. 1, pp. 1-18, 2018. [CrossRef] [Google Scholar] [Publisher Link]
[47] Timothy Richard Oke et al., *Urban Climates*, Cambridge University Press, 2017. [CrossRef] [Google Scholar] [Publisher Link]
[48] Bao-Jie He, and Lan Ding, and Deo Prasad, "Relationships among Local-Scale Urban Morphology, Urban Ventilation, Urban Heat Island and Outdoor Thermal Comfort under Sea Breeze Influence," *Sustainable Cities and Society*, vol. 60, 2020. [CrossRef] [Google Scholar] [Publisher Link]
[49] Fawzi Hicham Arrar et al., "Quantification of Outdoor Thermal Comfort Levels under Sea Breeze in the Historical City Fabric: The Case of Algiers Casbah," *Atmosphere*, vol. 13, no. 4, pp. 1-30, 2022. [CrossRef] [Google Scholar] [Publisher Link]
[50] Rongtao Wang et al., "Effects of Sky View Factor on Thermal Environment in Different Local Climate Zoning Building Scenarios-A Case Study of Beijing, China," *Buildings*, vol. 13, no. 8, pp. 1-22, 2023. [CrossRef] [Google Scholar] [Publisher Link]
[51] Tong Lyu, Riccardo Buccolieri, and Zhi Gao, "A Numerical Study on the Correlation between Sky View Factor and Summer Microclimate of Local Climate Zones," *Atmosphere*, vol. 10, no. 8, pp. 1-19, 2019. [CrossRef] [Google Scholar] [Publisher Link]
[52] Pooja Solanki, Lilly Rose Amirtham, and Chirag Deb, "Optimizing Sky View Factor and Vegetation to Mitigate Urban Heat in Hot-Humid Climates," *Discover Cities*, vol. 2, no. 1, pp. 1-25, 2025. [CrossRef] [Google Scholar] [Publisher Link]
[53] Erik Johansson, and Rohinton Emmanuel, "The Influence of Urban Design on Outdoor Thermal Comfort in the Hot, Humid City of Colombo, Sri Lanka," *International Journal of Biometeorology*, vol. 51, no. 2, pp. 119-133, 2006. [CrossRef] [Google Scholar] [Publisher Link]
[54] Rohinton Emmanuel, and Erik Johansson, "Influence of Urban Morphology and Sea Breeze on Hot Humid Microclimate: The Case of Colombo, Sri Lanka," *Climate Research*, vol. 30, no. 3, pp. 189-200, 2006. [CrossRef] [Google Scholar] [Publisher Link]

[55] Hongchi Zhang et al., "Spatial Differences in Thermal Comfort in Summer in Coastal Areas: A Study on Dalian, China," *Frontiers in Public Health*, vol. 10, pp. 1-18, 2022. [CrossRef] [Google Scholar] [Publisher Link]

[56] Wei Yang, Nyuk Hien Wong, and Steve Kardinal Jusuf, "Thermal Comfort in Outdoor Urban Spaces in Singapore," *Building and Environment*, vol. 59, pp. 426-435, 2013. [CrossRef] [Google Scholar] [Publisher Link]

[57] Juan A. Acero et al., "Measuring and Comparing Thermal Comfort in Outdoor and Semi-Outdoor Spaces in Tropical Singapore," *Urban Climate*, vol. 42, 2022. [CrossRef] [Google Scholar] [Publisher Link]

[58] A. Salvati et al., "Built Form, Urban Climate and Building Energy Modelling: Case-Studies in Rome and Antofagasta," *Journal of Building Performance Simulation*, vol. 13, no. 2, pp. 209-225, 2020. [CrossRef] [Google Scholar] [Publisher Link]

[59] Victorina Arif, and Lin Yola, "The Impact of Sky View Factor on Pedestrian Thermal Comfort in Tropical Context: A Case of Jakarta Sidewalk," *Sustainable Architecture and Building Environment: Proceedings of ICSDEMS 2020*, pp. 27-33, 2021. [CrossRef] [Google Scholar] [Publisher Link]

[60] T.R. Oke, "Canyon Geometry and the Nocturnal Urban Heat Island: Comparison of Scale Model and Field Observations," *Journal of Climatology*, vol. 1, no. 3, pp. 237-254, 1981. [CrossRef] [Google Scholar] [Publisher Link]

[61] Priyadarsini Rajagopalan, Kee Chuan Lim, and Elmira Jamei, "Urban Heat Island and Wind Flow Characteristics of a Tropical City," *Solar Energy*, vol. 107, pp. 159-170, 2014. [CrossRef] [Google Scholar] [Publisher Link]